



This is a repository copy of *Fast-flow signature in the stagnated Kamb Ice Stream, West Antarctica*.

White Rose Research Online URL for this paper:
<http://eprints.whiterose.ac.uk/92154/>

Version: Accepted Version

Article:

Ng, F. and Conway, H. (2004) Fast-flow signature in the stagnated Kamb Ice Stream, West Antarctica. *Geology*, 32 (6). 481 - 484. ISSN 0091-7613

<https://doi.org/10.1130/G20317.1>

Reuse

Unless indicated otherwise, fulltext items are protected by copyright with all rights reserved. The copyright exception in section 29 of the Copyright, Designs and Patents Act 1988 allows the making of a single copy solely for the purpose of non-commercial research or private study within the limits of fair dealing. The publisher or other rights-holder may allow further reproduction and re-use of this version - refer to the White Rose Research Online record for this item. Where records identify the publisher as the copyright holder, users can verify any specific terms of use on the publisher's website.

Takedown

If you consider content in White Rose Research Online to be in breach of UK law, please notify us by emailing eprints@whiterose.ac.uk including the URL of the record and the reason for the withdrawal request.



eprints@whiterose.ac.uk
<https://eprints.whiterose.ac.uk/>

Fast-flow signature in the stagnated Kamb Ice Stream, West Antarctica

Felix Ng

Department of Earth, Atmospheric and Planetary Sciences, Massachusetts Institute of Technology, Cambridge, Massachusetts 02139, USA

Howard Conway

Department of Earth and Space Sciences, University of Washington, Seattle, Washington 98195, USA

ABSTRACT

Among the major ice streams that drain West Antarctica, Kamb Ice Stream (formerly called Ice Stream C) is unique in that it stagnated ~150 yr ago, but its former fast-flow conditions are virtually unknown. Here we present surface-based radar profiles of the ice stream's undulating internal stratigraphy, which records these conditions. Our analysis of the profiles indicates that prestagnation flow velocities, averaged over a period <740 yr, exceeded $350 \text{ m}\cdot\text{yr}^{-1}$ in the trunk of the ice stream. This velocity constraint would be lower if the ice had been thickening (higher if thinning), but suggests mass loss from the ice-stream catchment that is of sufficient magnitude to reverse the gain estimated for today's Siple Coast region. Analysis of other ice streams would allow comparison of velocities over millennial time scales with observations of present-day velocities, useful for evaluating how West Antarctic ice drainage has evolved.

Keywords: West Antarctica, ice streams, radar, mass balance.

INTRODUCTION

Ice in the interior of the West Antarctic Ice Sheet flows slowly ($\sim 10 \text{ m}\cdot\text{yr}^{-1}$), but on its oceanward journey converges through tributaries into fast-flowing ($10^2\text{--}10^3 \text{ m}\cdot\text{yr}^{-1}$) ice streams. These ice streams exert strong control on ice-sheet mass balance through their changing activity (Shabtaie et al., 1988; Joughin et al., 1999, 2002; Conway et al., 2002; Joughin and Tulaczyk, 2002). Their behavior is therefore important for understanding ice-sheet contribution to global sea-level change, especially given concerns that West Antarctica, a marine ice sheet, may be prone to rapid collapse in the future (Alley and Bindschadler, 2001).

The stagnation of the trunk region of Kamb Ice Stream (Fig. 1) has received much attention (Rose, 1979; Retzlaff and Bentley, 1993; Anandakrishnan et al., 2001; Smith et al., 2002) for providing insights on ice-stream dynamics and because of ongoing debate as to whether it is evidence for ice-sheet stability or instability (Alley and Whillans, 1991). Zones of chaotic crevasses, caused by high strain rates (Vaughan, 1993), form at the lateral margins of ice streams today that are flowing faster than $\sim 100 \text{ m}\cdot\text{yr}^{-1}$ (Joughin et al., 1999, 2002). Prestagnation velocities of this magnitude are suggested for Kamb Ice

43 Stream by the existence of former (now buried) lateral margins (Retzlaff and Bentley,
44 1993; Smith et al., 2002), but a precise velocity estimate is needed to substantiate theories
45 about the cause and impact of stagnation. To explore other signatures of past flow
46 activity is essential.

47 In this paper we examine the internal stratigraphy of K2, the northern tributary of
48 Kamb Ice Stream (Fig. 1), revealed by three surface-based, low-frequency (2 MHz) radar
49 profiles (Fig. 2). Although the ice-stream trunk is nearly stagnant, velocities in the
50 tributaries are 60–80 m·yr⁻¹. Profile Z ($z-z'$) lies in the trunk and is just downstream of
51 the region of flow deceleration, where a bulge is growing (Price et al., 2001).

52 53 **RADAR OBSERVATIONS**

54 Radar-detected internal layers (Fig. 2) show remarkable lateral continuity,
55 implying that they are not necessarily destroyed by fast flow or its onset; other
56 measurements (not shown) confirm layer continuity downstream as well as across K2.
57 Continuous layering has been reported in other ground-based radar surveys on Kamb Ice
58 Stream and Whillans Ice Stream (Schultz et al., 1987; Wright et al., 1990; Jacobel et al.,
59 1993). In contrast, airborne radar data often reveal ice-stream internal structures to be
60 disrupted or unrecognizable (Bell et al., 1998; Siegert et al., 2003). We attribute such
61 disparity to different degrees of aliasing in the stacking procedure used to improve the
62 signal to noise ratio. Airborne systems employ a stacking distance similar to ours, but the
63 much higher bandwidth (typically ≥ 60 MHz) and proportionally lower wavelength make
64 them less able to resolve steeply dipping multiple layers. Many internal layers in K2 dip
65 at slopes >0.1 .

66 The internal layers in all three profiles undulate in a distinct trough-and-crest
67 sequence, depicting a pattern of folds whose axes are subparallel to ice flow and whose
68 amplitude increases with depth. The layers represent horizons of equal age (isochrones)
69 because low-frequency radar reflections in ice are due primarily to electrical conductivity
70 contrasts, likely inherited from snow deposition (Fujita et al., 2000). But isochrones are
71 not flow lines; nor do their ages offer direct clues for understanding layer deformation,
72 which registers cumulative shear strain. Numerous processes could have produced the
73 folds, including flow convergence or divergence in the ice-stream tributary system, flow
74 over bedrock bumps (Robin and Millar, 1982), nonuniform basal melting (Fahnestock et
75 al., 2001) or nonuniform surface accumulation (Vaughan et al., 1999); radar-detected
76 folds have also been hypothesized to result from changes in basal boundary conditions at
77 the onset of streaming (Jacobel et al., 1993). The spatiotemporal properties of such
78 processes within Kamb Ice Stream are uncertain, and their length scales may not
79 correspond to the dominant folding wavelength (on the order of kilometers). The origin
80 of the folds is unknown. Yet a simple analysis shows that they carry an important paleo-
81 streaming signature.

82 83 **ANALYSIS AND DISCUSSION**

84 We define 10 “flow bands” common to the profiles by using prominent crests (or
85 troughs) of the folds as lateral boundaries (Fig. 2). Folds are difficult to identify at depth,
86 due to radar attenuation, and near the surface, where their curvature is low and echoes
87 from buried crevasses interrupt the layers. We use a given fold if it can be traced in all

88 three profiles for more than a third of the ice thickness. Traces are extrapolated so that
89 flow bands extend from the ice surface to the bed.

90 Along flow, ice thickness decreases, accompanying an adverse bed-slope of the
91 tributary, but the width of each flow band decreases also (in approximately the ratio 3:2:1
92 in the profiles). The folds thus converge, and three independent explanations of this flow
93 signature (1 to 3 below) are relevant. In the following discussion we assume steady-state
94 flow in the study area (between profiles X and Z) before stagnation with a surface
95 geometry close to that of today. We also assume flow dominated by a basal velocity
96 component, because sliding at the ice-bed interface and/or subglacial till deformation
97 probably enabled the fast flow in the trunk and K2, as in the neighboring ice streams.

98 Straightforwardly, (1) transverse folds could have formed upstream of profile X
99 and entered the study area, where they encountered compression sideways together with
100 longitudinal stretching. Flow regimes like this are found in the upper reaches of active ice
101 streams. If the folds delivered at X were stationary, their axes would, in plan view,
102 coincide with flow lines.

103 Alternatively, there could have been no compression (or even expansion)
104 sideways in the study area, if downstream increase in flow velocity was less rapid than
105 envisaged in explanation 1. In this case, the signature can be explained by considering
106 that (2) the folds formed in the study area or (3) they were delivered at X while widening
107 in time. These two explanations are unlikely to dominate because the folds are
108 uncorrelated with bed topography or with bed changes; nonuniformities (such as in
109 surface accumulation or basal melting) between X and Z that could have generated
110 folding with the observed convergence are implausible; and there is no reason to expect
111 mechanisms acting in concert upstream to widen the folds being delivered. We regard the
112 signature as mainly due to the streaming regime in explanation 1, although its distortion
113 by time-varying flow or by folding processes in the study area cannot be excluded.
114 Modification and displacement of the profiles since stagnation began (~150 yr ago) are
115 limited and do not alter this conclusion.

116 Now, if we assume that the flow bands align with paleo-flow lines in plan view
117 and we ignore contributions from surface accumulation and basal melting, mass
118 conservation requires the flux through each flow band to be constant (Fig. 3). The ice
119 flux through cross section area A is $A \times u$, where u is area-averaged velocity. The area
120 ratios A_X/A_Y , A_Y/A_Z , and A_X/A_Z should therefore record the past-velocity ratios u_Y/u_X ,
121 u_Z/u_Y and u_Z/u_X respectively (subscript denotes radar profile). We measure areas from
122 Figure 2, but acknowledge that deviations of the profile normals from past flow direction
123 (likely to be $<30^\circ$) could overestimate area ratios by up to 15%. The area ratios for each
124 flow band exceed unity (Fig. 4), a result that points to a consistent downstream increase
125 in paleo-flow speed. When derived for the total area of the 10 flow bands, \hat{A} , the ratios
126 are $\hat{A}_X/\hat{A}_Y = 1.7 \pm 0.1$, $\hat{A}_Y/\hat{A}_Z = 2.3 \pm 0.1$ and $\hat{A}_X/\hat{A}_Z = 4.0 \pm 0.2$, which indicate $u_X:u_Y:u_Z \approx$
127 $1:1.7:4$. In addition, the presence of a buried lateral margin near km 35 of profile X
128 (Smith et al., 2002) suggests that $u_X \geq 100 \text{ m}\cdot\text{yr}^{-1}$ prior to stagnation. Combining this
129 inference with the fourfold velocity increase from X to Z provides the first indication that
130 prestagnation velocities in the trunk exceeded $350 \text{ m}\cdot\text{yr}^{-1}$ (conservative lower bound,
131 based on 30° deviation). Because paleo-flow speeds in the range 10^2 – $10^3 \text{ m}\cdot\text{yr}^{-1}$ are
132 plausible, the velocity long-profile established here is consistent with such profiles
133 observed on active ice streams (e.g., the upstream region of Whillans Ice Stream).

134 Our results are consistent also with regard to cross-tributary variation in velocity.
 135 Rising ratios across Figure 4 imply greater (multiplicative) change in paleo-flow speed to
 136 the north, culminating in flow band 10. A simple reason is that on X, flow band 10 is
 137 within a few kilometers of the former shear margin, where u_X would have been
 138 substantially less than its midtributary value. On the other hand, the flow bands on Z lie
 139 >10 km south of the margin, so we expect u_Z to have been more uniform. In this
 140 interpretation, short-range fluctuations in the ratios reflect variations in velocity and in
 141 fold delivery as well as other distortions of the signature.

142 The steady-state assumption imposes restrictions on our estimates of velocity ratio
 143 and of velocity (often called “balance velocity” [Paterson, 1994] for such an assumption).
 144 The transit time of ice in the study area is 740 yr for a mean paleovelocity of $(350 +$
 145 $100)/2 \text{ m}\cdot\text{yr}^{-1}$. Thus, our estimates apply within <740 yr before stagnation. Although it is
 146 unknown how flow velocities had varied over this period, thinning or thickening in the
 147 study area would, respectively, raise or lower the estimates. No attempt is made to
 148 increase our minimum velocity by prescribing local thinning with basin-wide mass loss
 149 (discussed below). Further, we emphasize the uncertainties in using buried margins to
 150 infer absolute velocity. In the Siple Coast, crevassed shear margins develop today where
 151 the centerline flow speed of ice streams exceeds $100 \text{ m}\cdot\text{yr}^{-1}$ (Joughin et al. [1999, 2002];
 152 see also Whillans et al. [2001, p. 265] for Whillans Ice Stream, and Smith et al. [2002]
 153 for Bindschadler Ice Stream). Our starting threshold is based on this observation, and not
 154 on a physical model of shear margins and critical stresses to initiate crevassing. However,
 155 since the study area is now free of surface crevasses, we consider later the effect of
 156 lowering the threshold to $60 \text{ m}\cdot\text{yr}^{-1}$ (present-day flow speed at X), which leads to more
 157 conservative results.

158 Otherwise two factors reinforce our velocity constraint ($\geq 350 \text{ m}\cdot\text{yr}^{-1}$). First, basal
 159 melting rates ($\sim 0.01 \text{ m}\cdot\text{yr}^{-1}$) are unlikely to exceed surface accumulation rates (today ~ 0.1
 160 $\text{m}\cdot\text{yr}^{-1}$ ice-equivalent). In the flux balance, contribution of these rates to the through-flux
 161 would raise our trunk velocity estimate by $\sim 10\%$ (under the assumption that $u_X \approx 100$
 162 $\text{m}\cdot\text{yr}^{-1}$ and net accumulation is $\sim 0.1 \text{ m}\cdot\text{yr}^{-1}$). Second, profile Z has probably undergone
 163 poststagnation shortening along flow, as evidenced by bulge formation in its vicinity
 164 (Price et al., 2001), and downscaling of A_Z to account for this further increases the ratio
 165 u_Z/u_X .

166 Inactivity of Kamb Ice Stream is currently responsible for $+20.5 \pm 3.1$ gigatons
 167 per year ($\sim 70\%$) of the positive mass balance of the Siple Coast region of West Antarctica
 168 (26.8 ± 14.9 gigatons per year) (Joughin and Tulaczyk, 2002). Although our velocity
 169 constraint remains a lower bound, it differs sufficiently from the crevasse-based estimate
 170 ($\geq 100 \text{ m}\cdot\text{yr}^{-1}$) to be important. Our constraint indicates negative mass balance for the
 171 active Kamb Ice Stream system, because $350 \text{ m}\cdot\text{yr}^{-1}$ streaming velocities across the trunk
 172 near Upstream C camp (UpC in Fig. 1) would result there in a discharge of ~ 28 gigatons
 173 per year, roughly twice the accumulation upstream. (This calculation assumes plug-flow
 174 along an 80 km wide trunk and a 1.1 km mean ice thickness.) Indeed, such discharge may
 175 reverse the present-day regional balance and could have dominated that of the past. These
 176 outcomes remain possible even if the crevasse threshold is $60 \text{ m}\cdot\text{yr}^{-1}$ (paleo-velocities
 177 and discharge reduced by 40%), owing to large accumulation-rate uncertainties in the
 178 mass-balance estimates.

179 Knowledge of prestagnation velocity is crucial for understanding the
 180 thermomechanics of Kamb Ice Stream (Raymond, 2000; Joughin et al., 2002). This study
 181 provides a new observational context for assessing earlier estimates, none of which
 182 derives from signatures of past flow. Where models assume the ice stream in steady state,
 183 estimated velocities near UpC (e.g., $\sim 200 \text{ m}\cdot\text{yr}^{-1}$, Joughin et al. [2003]) can be expected
 184 to be less than $350 \text{ m}\cdot\text{yr}^{-1}$ due to the balance implication of the latter value. Other models
 185 have explored the spatial dynamics of the stagnation process (Fastook, 1987; Bougamont
 186 et al., 2003). Although our signature is a time-integrated phenomenon, it will be of
 187 interest to test simulated velocities against it by introducing flow markers in such models.
 188 Meanwhile, our finding of long-term mass loss seems to support mechanisms that invoke
 189 ice-stream thinning and resulting changes in basal regime to trigger stagnation (e.g.,
 190 Bougamont et al., 2003). Strong motivations exist for extending the radar analysis.
 191 Although the nature of the coherent internal structures exploited here is not fully
 192 understood, our results highlight new opportunities for deciphering ice-stream history and
 193 organization.

194

195 **ACKNOWLEDGMENTS**

196 We thank A. Gades for running the radar survey; M. Conway, N. Lord, and B.
 197 Smith for field assistance; I. Joughin and S. Price for providing velocity data and the base
 198 image of Figure 1; and C.R. Bentley, T. Murray, and C.F. Raymond for insight and
 199 contributions. We also thank N. Iverson and S. Tulaczyk for critical reviews. This work
 200 was supported by a Royal Society Fulbright Postdoctoral Science Fellowship and a
 201 M.I.T. Leavitt Research Fellowship (to Ng), and by the U.S. National Science
 202 Foundation.

203

204 **REFERENCES CITED**

- 205 Alley, R.B., and Whillans, I.M., 1991, Changes in the West Antarctic ice sheet: *Science*,
 206 v. 254, p. 959–963.
- 207 Alley, R.B., and Bindschadler, R.A., 2001, The West Antarctic ice sheet and sea-level
 208 change, *in* Alley, R.B., and Bindschadler, R.A., eds., *The West Antarctic Ice*
 209 *Sheet: Behavior and environment: American Geophysical Union Antarctic*
 210 *Research Series*, v. 77, p. 1–11.
- 211 Anandakrishnan, S., Alley, R.B., Jacobel, R.W., and Conway, H., 2001, The flow regime
 212 of Ice Stream C and hypotheses concerning its recent stagnation, *in* Alley, R.B.,
 213 and Bindschadler, R.A., eds., *The West Antarctic Ice Sheet: Behavior and*
 214 *environment: American Geophysical Union Antarctic Research Series*, v. 77,
 215 p. 283–294.
- 216 Bell, R.E., Blankenship, D.D., Finn, C.A., Morse, D.L., Scambos, T.A., Brozena, J.M.,
 217 and Hodge, S.M., 1998, Influence of subglacial geology on the onset of a West
 218 Antarctic ice stream from aerogeophysical observations: *Nature*, v. 394, p. 58–62.
- 219 Bougamont, M., Tulaczyk, S., and Joughin, I., 2003, Response of subglacial sediments to
 220 basal freeze-on: 2. Application in numerical modeling of the recent stoppage of
 221 Ice Stream C, West Antarctica: *Journal of Geophysical Research*, v. 108, no. B4,
 222 2223, doi: 10.1029/2002JB001936.

- 223 Conway, H., Catania, G., Raymond, C.F., Gades, A.M., Scambos, T.A., and Engelhardt,
224 H., 2002, Switch of flow direction in an Antarctic ice stream: *Nature*, v. 419,
225 p. 465–467.
- 226 Fahnestock, M., Abdalati, W., Joughin, I., Brozena, J., and Gogineni, P., 2001, High
227 geothermal heat flow, basal melt, and the origin of rapid ice flow in central
228 Greenland: *Science*, v. 294, p. 2338–2342.
- 229 Fastook, J.L., 1987, Use of a new finite element continuity model to study the transient
230 behavior of Ice Stream C and causes of its present low velocity: *Journal of*
231 *Geophysical Research*, v. 92, p. 8941–8949.
- 232 Fujita, S., Matsuoka, T., Ishida, T., Matsuoka, K., and Mae, S., 2000, A summary of the
233 complex dielectric permittivity of ice in the megahertz range and its applications
234 for radar soundings, *in* Hondoh, T., ed., *Physics of ice core records*: Sapporo,
235 Japan, Hokkaido University Press, p. 185–212.
- 236 Gades, A.M., 1998, Spatial and temporal variations of basal conditions beneath glaciers
237 and ice sheets inferred from radio echo sounding measurements [Ph.D. thesis]:
238 Seattle, University of Washington, 192 p.
- 239 Jacobel, R.W., Gades, A.M., Gottschling, D.L., Hodge, S.M., and Wright, D.L., 1993,
240 Interpretation of radar-detected internal layer folding in West Antarctic ice
241 streams: *Journal of Glaciology*, v. 39, p. 528–537.
- 242 Joughin, I., and Tulaczyk, S., 2002, Positive mass balance of the Ross Ice Streams, West
243 Antarctica: *Science*, v. 295, p. 476–480.
- 244 Joughin, I., Gray, L., Bindschadler, R., Price, S., Morse, D., Hulbe, C., Mattar, K., and
245 Werner, C., 1999, Tributaries of West Antarctic ice streams revealed by
246 RADARSAT interferometry: *Science*, v. 286, p. 283–286.
- 247 Joughin, I., Tulaczyk, S., Bindschadler, R., and Price, S.F., 2002, Changes in West
248 Antarctic ice stream velocities: Observation and analysis: *Journal of Geophysical*
249 *Research*, v. 107, no. B11, 2289, doi: 10.1029/2001JB001029.
- 250 Joughin, I.R., Tulaczyk, S., and Engelhardt, H.F., 2003, Basal melt beneath Whillans Ice
251 Stream and Ice Streams A and C, West Antarctica: *Annals of Glaciology*, v. 36,
252 p. 257–262.
- 253 Paterson, W.S.B., 1994, *The physics of glaciers*: Oxford, Great Britain, Pergamon, 480 p.
- 254 Price, S.F., Bindschadler, R.A., Hulbe, C.L., and Joughin, I.R., 2001, Post-stagnation
255 behavior in the upstream regions of Ice Stream C, West Antarctica: *Journal of*
256 *Glaciology*, v. 47, 283–294.
- 257 Raymond, C.F., 2000, Energy balance of ice streams: *Journal of Glaciology*, v. 46,
258 p. 665–674.
- 259 Retzlaff, R., and Bentley, C.R., 1993, Timing of stagnation of Ice Stream C, West
260 Antarctica, from short-pulse radar studies of buried surface crevasses: *Journal of*
261 *Glaciology*, v. 39, p. 553–561.
- 262 Robin, G. de Q., and Millar, D.H.M., 1982, Flow of ice sheets in the vicinity of
263 subglacial peaks: *Annals of Glaciology*, v. 3, p. 290–294.
- 264 Rose, K.E., 1979, Characteristics of ice flow in Marie Byrd Land, Antarctica: *Journal of*
265 *Glaciology*, v. 24, p. 63–75.
- 266 Schultz, D.G., Powell, L.A., and Bentley, C.R., 1987, A digital radar system for echo
267 studies on ice sheets: *Annals of Glaciology*, v. 9, p. 206–210.

- 268 Shabtaie, S., and Bentley, C.R., 1987, West Antarctic ice streams draining into the Ross
 269 Ice Shelf: Configuration and mass balance: *Journal of Geophysical Research*,
 270 v. 92, p. 1311–1336.
- 271 Shabtaie, S., Bentley, C.R., Bindschadler, R.A., and MacAyeal, D.R., 1988, Mass-
 272 balance studies of Ice Streams A, B, and C, West Antarctica, and possible surging
 273 behavior of Ice Stream B: *Annals of Glaciology*, v. 11, p. 137–149.
- 274 Siegert, M.J., Payne, A.J., and Joughin, I., 2003, Spatial stability of Ice Stream D and its
 275 tributaries, West Antarctica, revealed by radio-echo sounding and interferometry:
 276 *Annals of Glaciology*, v. 37, p. 377–382.
- 277 Smith, B.E., Lord, N.E., and Bentley, C.R., 2002, Crevasse ages on the northern margin
 278 of Ice Stream C, West Antarctica: *Annals of Glaciology*, v. 34, p. 209–216.
- 279 Vaughan, D.G., 1993, Relating the occurrence of crevasses to surface strain rates: *Journal*
 280 *of Glaciology*, v. 39, p. 255–266.
- 281 Vaughan, D.G., Corr, H.F.J., Doake, C.S.M., and Waddington, E.D., 1999, Distortion of
 282 isochronous layers in ice revealed by ground-penetrating radar: *Nature*, v. 398,
 283 p. 323–326.
- 284 Whillans, I.M., Bentley, C.R., and Van der Veen, C.J., 2001, Ice Streams B and C, *in*
 285 Alley, R.B., and Bindschadler, R.A., eds., *The West Antarctic Ice Sheet: Behavior*
 286 *and environment: American Geophysical Union Antarctic Research Series*, v. 77,
 287 p. 257–281.
- 288 Wright, D.L., Hodge, S.M., Bradley, J.A., Grover, T.P., and Jacobel, R.W., 1990,
 289 *Instruments and methods: A digital low-frequency, surface-profiling ice-radar*
 290 *system: Journal of Glaciology*, v. 36, p. 112–121.

291

292 **FIGURE CAPTIONS**

293 Figure 1. Kamb Ice Stream (KIS), including its now-stagnant main trunk and tributaries
 294 K1 and K2. Hatched areas are relict margins mapped by airborne radar surveys (Shabtaie
 295 and Bentley, 1987). Flow direction is from top left to bottom right. Color code shows
 296 present-day surface flow speeds from Joughin and Tulaczyk (2002); gray regions lack
 297 data coverage. White lines locate radar profiles of Figure 2: $x-x'$, $y-y'$, and $z-z'$, referred
 298 to also as X, Y, and Z for convenience. End coordinates are 82.15°S 124.66°W (x),
 299 81.78°S 125.44°W (x'), 82.16°S 128.02°W (y), 81.90°S 128.46°W (y'), 82.24°S 136.00°W
 300 (z), 82.07°S 136.00°W (z'). Other labels are old Upstream C camp (UpC), Whillans Ice
 301 Stream (WIS, formerly Ice Stream B) and Bindschadler Ice Stream (BIS, formerly Ice
 302 Stream D). Inset shows study-area location in Antarctica.

303 Figure 2. Ice-penetrating radar profiles along $x-x'$ (X, top), $y-y'$ (Y, middle) and $z-z'$ (Z,
 304 lower) show internal layers and bed. Flow direction is into page. Top panel depicts data
 305 in gray-scale; middle and lower panels show continuous traceable layers. Data were
 306 acquired with a short-pulse system (detailed by Gades [1998]) operating at a center
 307 frequency of 2 MHz. Depth resolution is ~21 m (quarter-wavelength); upper tens of
 308 meters (black band in profile X) are not resolved. Data were recorded every 52 m (along
 309 profiles X and Y) and 26.5 m (profile Z). Each record consists of several hundred stacked
 310 (averaged) waveforms to improve signal to noise ratio. Additional processing includes
 311 filtering, corrections for surface topography, migration, and conversion of two-way
 312 traveltime to depth, taking into account higher wave velocities in near-surface snow.

313 Folding pattern at X is seen downstream at Y and Z. We trace prominent troughs and
 314 crests of folds from X to Y to Z, as well as in each profile (where no longer visible,
 315 extrapolating traces vertically), in order to define flow bands discussed in text.

316 Figure 3. Model relationship between internal layers and steady flow of actively
 317 streaming ice. Flow velocity is independent of depth but may vary cross-stream and
 318 downstream. Layer undulations show correspondence between two profiles $x-x'$ and $z-z'$
 319 and are assumed invariant in horizontal position when being delivered at $x-x'$ so that, in
 320 plan view, their crests (or troughs) coincide with flow lines. Vertical lines demarcate
 321 boundaries of a flow band. Mass conservation requires outflux of ice ($A_Z u_Z$) to equal
 322 influx ($A_X u_X$) plus net accumulation (neglected in analysis).

323 Figure 4. Area ratios A_X/A_Y , A_Y/A_Z , and A_X/A_Z for flow bands as proxies for ratios of
 324 paleo-streaming velocities u_Y/u_X , u_Z/u_Y and u_Z/u_X . Arrows on right indicate ratios for
 325 flow bands combined, \hat{A}_X/\hat{A}_Y , \hat{A}_Y/\hat{A}_Z , and \hat{A}_X/\hat{A}_Z . Error bars derive from upper and lower
 326 estimates of area for each flow band, based on horizontal range of crests (or troughs)
 327 identified in Figure 2. These errors exceed the errors on the area ratios given in text
 328 because each flow band is much smaller than area of 10 flow bands combined.

329

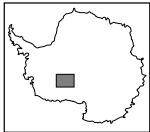
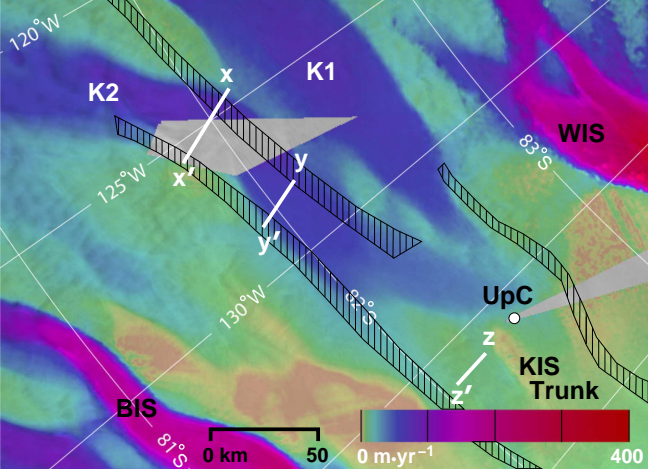


Fig. 1
Ng and Conway

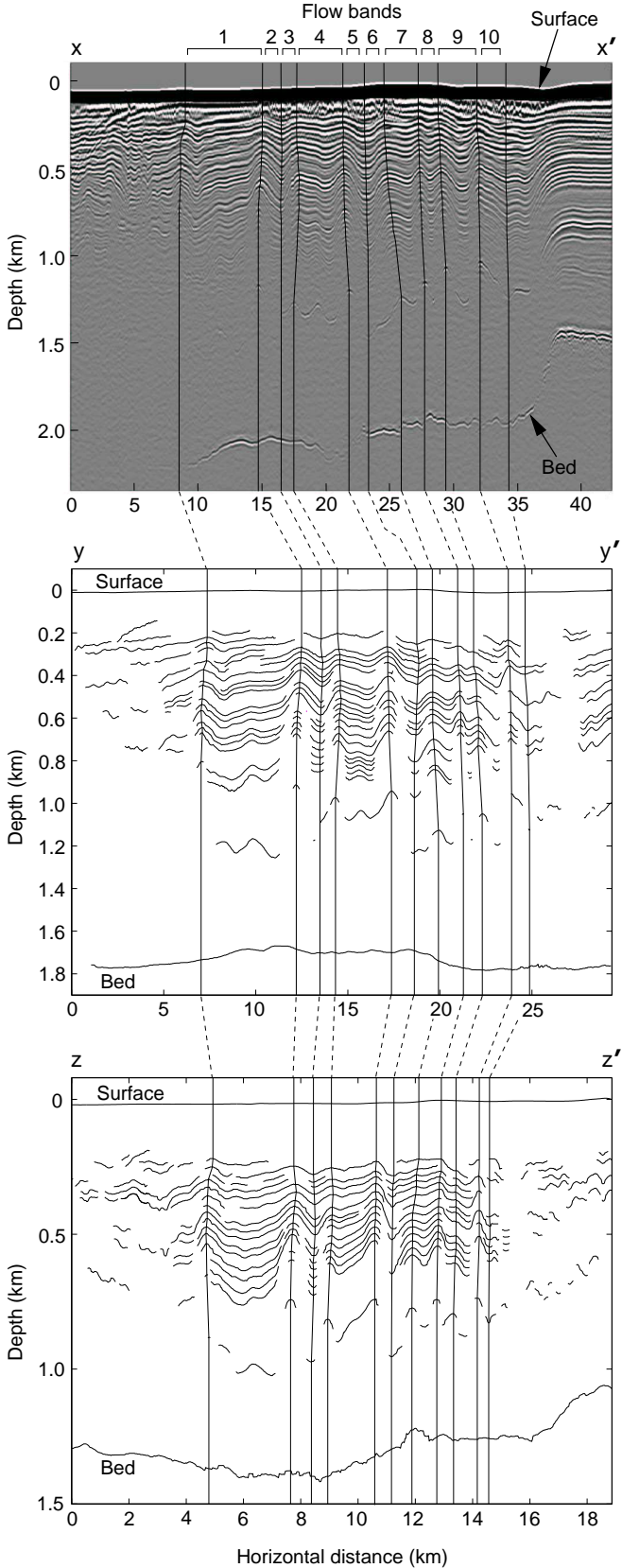


Fig. 2
Ng and Conway

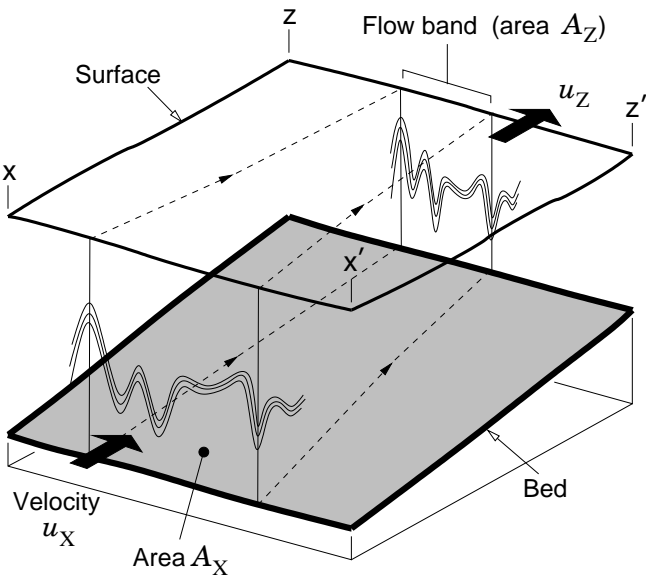


Fig. 3
Ng and Conway

Area ratios

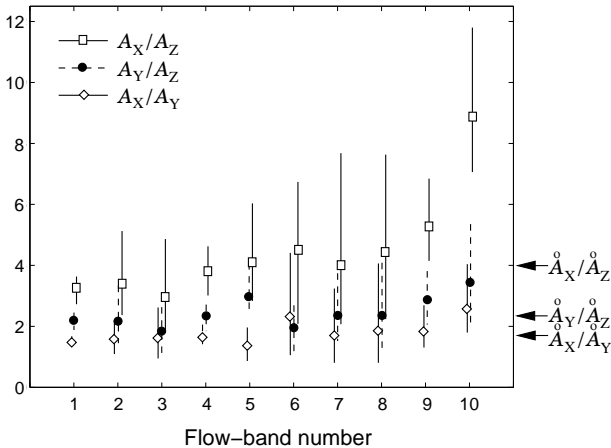


Fig. 4
Ng and Conway